ACTIVE DOSIMETER FOR MEASUREMENT OF THE RADIATION ENVIRONMENT IN A HUMAN PHANTOM ON BOARD THE INTERNATIONAL SPACE STATION

J. Semkova [(1)], G. Todorova [(1)], R. Koleva [(1)], N. Kanchev [(1)], V. Petrov [(2)], V. Shurshakov [(2)], V. Benghin[(2)], I. Tchhernykh [(2)], Yu. Akatov [(2)], V. Redko [(2)], Yu. Ivanov [(2)].

(1) Solar-Terrestrial Influences Laboratory, Bulgarian Academy of Sciences, Acad. G. Bonchev Str. Block 3, 1113, Sofia, Bulgaria, e-mail: jepero@vmsys.stil.acad.bg

(2) Institute of Biomedical Problems, State Research Center of Russia, Khoroshovskoye sh. 76-A, 123007, Moscow, Russia, e-mail: srag@pike.net.ru

Abstract - *Described is the Liulin-5 active dosimetric telescope designed for measurement of the depth distribution of the space radiation doses in a human phantom on the Russian Segment of the International Space Station (ISS.). Liulin-5 is a part of the international project MATROSHKA-R on ISS. Energy deposition spectra, linear energy transfer spectra, flux and dose rates for charged particles will be measured simultaneously with near real time resolution at 3 different depths of the phantom by means of 3 silicon detectors. The aim of Liulin-5 experiment is long term (4-5 years) investigation of the radiation environment dynamics inside the phantom, mounted in different compartments. Presented is the current status of the new device. Presented are the test results of the laboratory prototype unit. Liulin-5 will be flown on the ISS in 2002.*

Keywords - ionizing radiation, space, measurement**.**

1. INTRODUCTION

During space flights cosmonauts are exposed to space radiation. Experience having been gained for the previous period of space exploration allows coming to the only conclusion that a space flight is a human activity of a high radiation hazard level.

The major sources of radiation in space can be divided into two big classes: primary and secondary radiation. Primary radiation permanently exists in space and is one of its specific characteristics. Secondary radiation appears as a result of nuclear reactions of the primary radiation with the matter.

The primary radiation field in the space consists of the galactic cosmic rays (GCR), solar cosmic rays (SCR) and Earth radiation belts (ERB). At the orbit of ISS the main part of the primary radiation field is due to GCR and the trapped protons of the ERB. Previous flight measurements [1] have shown that the relatively small number (compared to trapped particles) of GCR heavy ions contributes 40% or more of the dose equivalent at the ISS inclination.

Interaction of the primary radiation field with the hull of the spacecraft results in a complex secondary radiation field consisting of charged particles, neutrons, gamma and x-rays, as well μ- and π-mesons. Considerable component of that field are particles of high linear energy transfer (LET), resulting in very high biological effectiveness. In addition it is characterized by nonuniform dose distribution as by a body depth as with time.

Because the highly ionizing nature of the heavy ions even a single particle traversal can produce deleterious biological effects such as cell transformation and DNA damage [2]-a single particle traversal can kill or, what may be worse, severely damage a cell, eventually leading to cancer. Such “late effects” caused by GCR heavy ions have been identified by the National Research Council [3] as the principal radiation risk to astronauts on extended stays outside low earth orbit, and many of the same concerns apply to the ISS. Where single particle effects are important, identification of these particles is essential to evaluating crew radiation exposures—in other words, not just absorbed dose, but dose equivalent, or absorbed dose weighted by biological effectiveness, must be determined.

The ISS internal radiation environment will be complex, with incident external space radiation field modulated by widely varying amounts of shielding and internal material, including the astronaut’s bodies.

For the estimation of the organ doses, and thus the radiation risk, measurements in human phantoms are essential [4].

The experiment MATROSHKA-R is aimed to study the depth dose distribution at the sites of critical organs of the human body, using models of human body-anthropomorphic and spherical tissue–equivalent phantoms [5]. The MATROSHKA-R experiment envisages long term measurements of absorbed and equivalent dose rates from all space radiation sources in different points inside the phantoms located on the ISS external surface and inside the station, measurements of the radiation spectral and angular distributions inside and outside ISS.

ISBN 972-98115-4-7 © 2001 IT

2. SPHERICAL TISSUE–EQUIVALENT PHANTOM

The spherical phantom consists of 13 tissue–equivalent layers. The diameter of the phantom is 350 mm, and the weight is 30 kg. The layers beside the central have cylindrical openings, where passive dosimeters will be placed. The central layer has 4 perpendicular channels. Inside 3 of them dosimetric containers will be placed. Inside the largest channel will be placed Liulin-5 dosimeter. On the outer surface of the phantom passive dosimeters will be also placed.

3. LIULIN-5 DESCRIPTION

Liulin-5 is a further development of the Liulin active dosimeter [6,7], variants of which flew for several years on the Mir space station.

3.1 Liulin-5 modules

Liulin-5 consists of 2 units: detector module, placed inside the phantom and electronic block outside it (Fig.1).

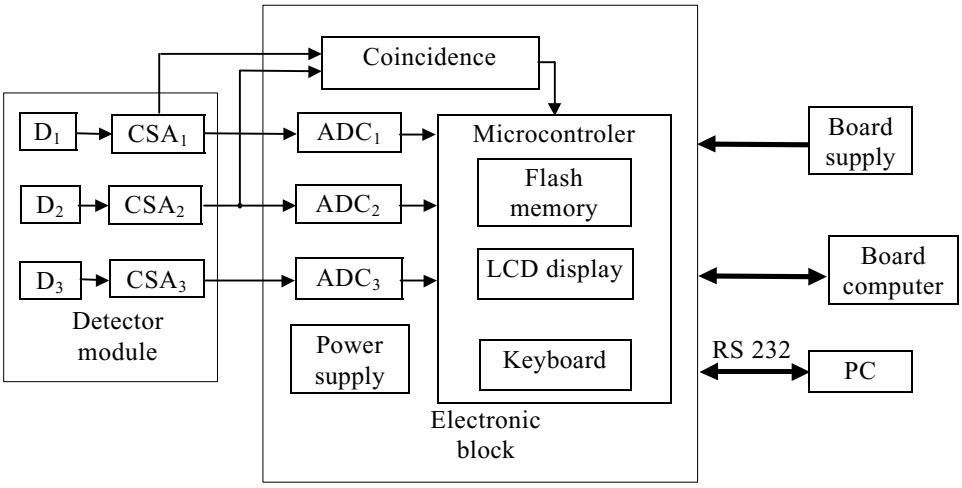

Fig.1 - Block-diagram of Liulin-5.

Detector module will be mounted in a container in the form of a tube of dimensions 175x50 mm. Detector module contains 3 silicon detectors D_1-D_3, placed at different depths to measure the dose depth distribution, and 3 charge sensitive preamplifiers-shaping amplifiers (CSA_1-CSA_3). First one of the detectors is placed near the phantom surface and the third detector is placed at the center of the spherical phantom. The detectors are arranged as a telescope.

The electronic block is mounted outside the phantom. It provides the supply to the detector module, controls the operation of Liulin-5 and accumulates the data from 24 hours measurement in flash memory. Liulin-5 transmits data to the board computer once a day. Maximum volume of data transmitted is 5 Mbyte/day. Two step pulse height amplification and following AD conversion (ADC_1-ADC_3) is used to measure the energy loss spectra in each one of the detectors with a dynamic range of 3300. Real-time clock, keyboard and visual display are incorporated in the electronic module for the instrument operation control. Coincidence technique is used to provide directional information and define the path length of particles through the first detector and to separate the coincidence events in the first and second detectors, which allow defining the LET in the first one of detectors.

3.2 Functional diagram

The functional diagram, which illustrates measurement of the signals, corresponding to the particle flux and energy loss spectra in first one of detectors and coincidence events both in first and second detector is shown in Fig. 2. The detectors D_1 and D_2 are connected to CSA_1 and CSA_2 respectively. There are 2 outputs of CSA_1-output of the charge -sensitive preamplifier (timing pulse of V_1 amplitude) and output of the shaping amplifier. The amplitudes V_1 and V_2 of these pulses are proportional to the energy loss of each particle penetrating the first detector. Timing output signal controls the discriminators.

The thresholds of two discriminators define the low limits of two sub -ranges of measurement the energy loss spectrum in the same detector. The threshold V_{ref1} of the first discriminator defines the low limit of the low sub-range of energy loss spectrum (LELS) measurement in the first detector. The threshold V_{ref2} of the second discriminator defines the low limit of the high sub-range spectrum measurement (HELS). The output signals of the discriminators control the gating logic of ADC_1.

An analog multiplexer provides signals of V_2. amplitudes in the range 0.0235-6 V at the input of ADC_1. These signals represent the output pulses of the shaping amplifier of CSA_1/or output pulses of the following pulse amplifier. The number of ADC_1 output pulses at the end of conversion time corresponds to V_2 amplitude and defines the

relevant spectral channel. This number (channel) is in the range 1-256 for LELS and in the range 17-256 for HELS.

The measurement of the signals, corresponding to the particle flux and energy loss spectra in detectors D_2 and D_3 is the same as for detector D_1.

Two coincidence schemes define the coincidence signals from the discriminators of two sub-range of measurement of CSA_1 and CSA_2.

The microcontroler accumulates the data for particle flux, energy loss spectra and absorbed dose rate measured in each of detectors. The measured parameters can be displayed and monitored on LCD display by the operator commands.

Different operational modes are pre-programmed. Switching between modes is automatically or manually. The output data contains time of the measurement, operational mode and measured data.

3.3 Timing diagram

The timing-diagram, which illustrates the measurement, as described in the functional diagram of Liulin-5 is shown in Fig. 3.

Panel 1 shows the timing pulses V_1 of CSA_1 and the thresholds $Vref_1$, $Vref_2$ of the respective discriminators, connected to the timing output of CSA_1.

Panel 2 shows the formed output signals of the discriminator of $Vref_1$ threshold. The number of these signals for a given time corresponds to the particle flux F_1 in the first detector.

Panel 3 shows the formed output signals of the discriminator of $Vref_2$ threshold. The number of these signals for a given time corresponds to the high sub-range particle flux F_{1H} in the same detector.

Panel 4 represents the pulses V_2 at the input of ADC_1.

On panel 5 are the output signals of ADC_1. The total number d_1 of these pulses for a given time corresponds to the absorbed dose for the same time.

Panel 6 shows the timing pulses V_3 of CSA_2 and the thresholds $Vref_3$, $Vref_4$ of the respective discriminators.

Panels 7 and 8 show the signals corresponding to the particle flux F_2 respectively F_{2H} in the second detector.

Panel 9 shows the coincidence events in both detectors and the flux F_C of these events.

Panel 10 shows the coincidence events in the high sub-range of measurement of both detectors and the flux F_{CH} of these events.

3.4 Liulin-5 parameters

The parameters, measured by each of detectors of Liulin-5 are as follows:

- Absorbed dose rate in the range 0.04 $x10^{-6}$ Gy/h - 0,6 Gy/h;
- Intensity of the particle flux in the range 0 - 10^3 particle/(cm^2.sec);
- Energy loss spectrum in the range 0.1-20 MeV in 256 channels (LELS); Energy loss spectrum in the range 20-200 MeV in 240 channels (HELS).

LET is calculated only for coincidence events both in first and second detectors. LET spectrum is constructed in 256 channels for LELS and in 240 channels for HELS.

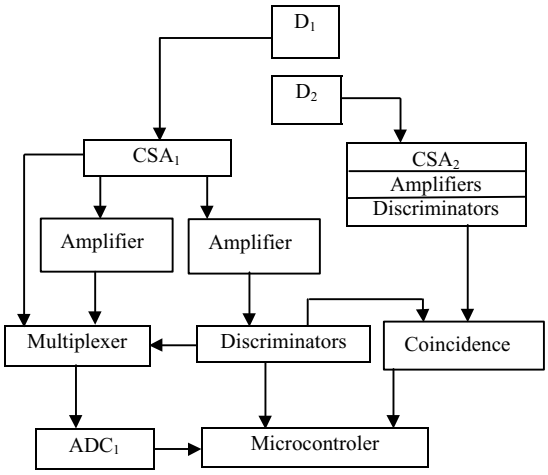

Fig. 2 Functional diagram

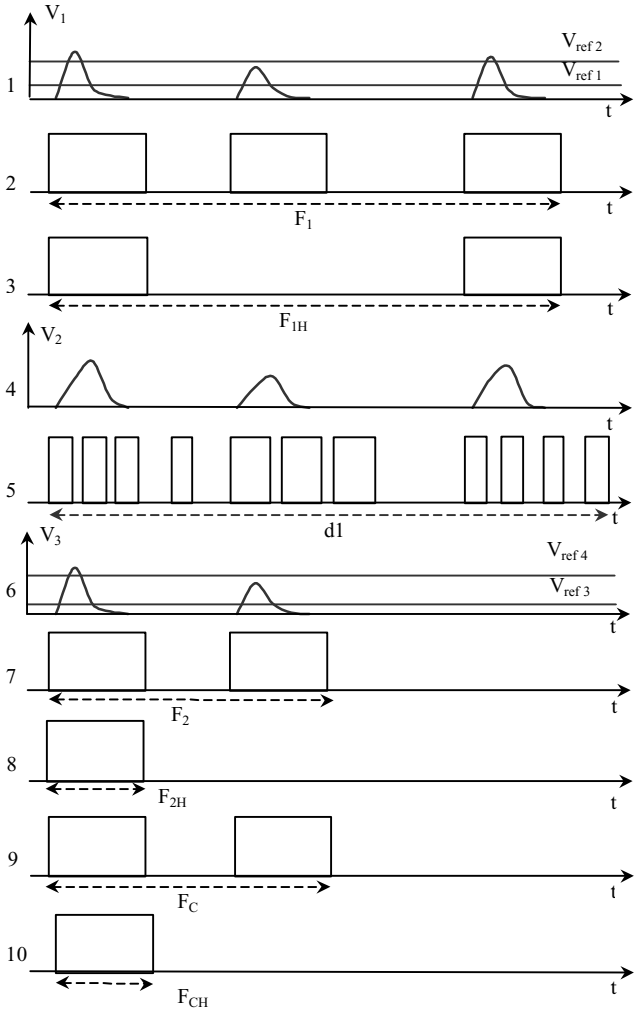

Fig. 3. Timing diagram

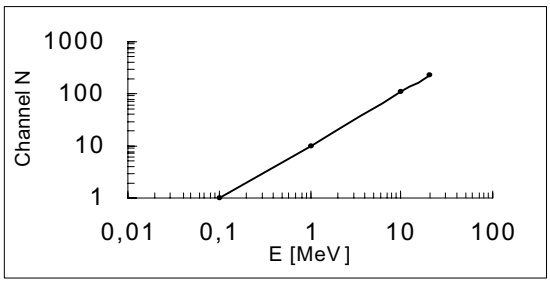

Fig. 4a - Electrical test results in the sub - range 0.1 - 20 MeV.

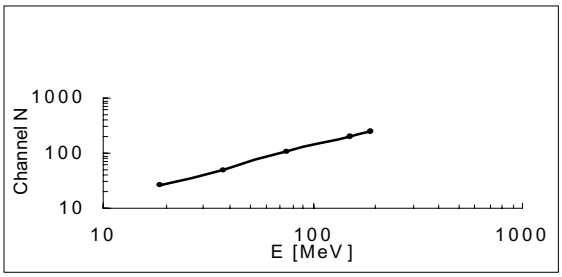

Fig. 4b - Electrical test results in the sub-range 20-200 MeV

4. LABORATORY TESTS

A laboratory prototype of a solid state dosimetric telescope, consisting of two detectors has been developed [8] and tested to measure energy loss spectrum, LET spectrum, flux and dose rate. The thickness of the first detector is 2 mm and the thickness of the second detector is 0.5 mm. The distance between the detectors is 20 mm. The telescope geometry allows ±8% accuracy of LET calculation. The thresholds of the discriminators were set to 120 keV.

4.1 Electrical tests

In Fig. 4a and Fig. 4b are presented the results of the electrical calibration of the prototype in 2 sub-ranges of the energy deposition range. The amplitude of the test signal at the input of the charge sensitive preamplifier simulates the energy deposition in the detector. On x-axes are presented the simulated energy losses in the detector, on y-axes are the respective channels of the ADC. The accuracy of the measurement is within ±2% of the calculated values.

4.2 Initial testing with laboratory radioactive sources

Initial testing of the laboratory prototype was performed using ^{60}Co, ^{137}Cs and α sources. The ^{60}Co and ^{137}Cs sources were placed in front of the first detector at distance about 15 mm. α source was placed in front of the first detector at distance about 2 mm.

In Fig. 5 the energy loss spectra of ^{60}Co in both detectors of the telescope and the spectrum of the coincidence events are presented. The time of the measurement was 60 s. The spectrum of coincidence events was used to calculate the LET. LET value is below 0.5 keV/μm, which is typical for a gamma source.

In Table 1 the results of measurement of particle flux respectively from first (F_1) and second detectors (F_2) and coincidence events are presented. Only a part of the particles penetrating the second detector form coincidences. α-particles do not penetrate the second detector. It is seen that no spurious coincidence events were registered during tests with α-source. The last column presents the flux of the gamma background, measured by the first detector.

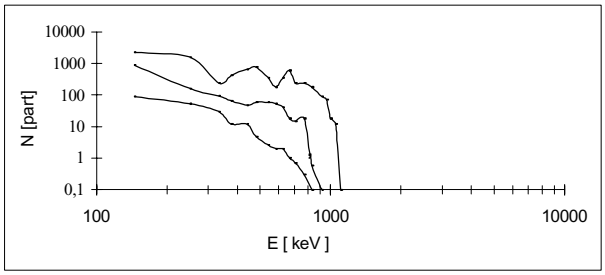

Fig. 5 - Energy loss spectrum of ^{60}Co in: the first detector of the telescope (upper curve), the second detector of the telescope (middle curve) and energy loss spectrum in the first detector of the particles forming coincidences (lower curve).

Table 1-Results of testing with different radioactive sources

Source	F_1 [particle/s]	F_2 [particle/s]	Coincidence [particle/s]	Gamma background [particle/s]
^{60}Co	150	10.7	4.5	0.2
^{137}Cs	5106	29	4	0.1
α	4788	0.1	0	0.1

5. CONCLUSIONS

Developed is the Liulin-5 active dosimetric telescope designed for long-term measurements of radiation environment parameters inside a tissue equivalent phantom on ISS.

The results of the electrical calibration of the laboratory model of Liulin-5 in 2 sub-ranges of the energy deposition range show that the accuracy of the measurement is within ±2% of the calculated values.

The tests of the laboratory model of Liulin-5 with laboratory radioactive sources show that the maximum energy deposition of gamma sources in each of the detectors of the telescope is about 1 MeV. The value of LET is below 0.5 keV/μm. Spurious penetrating in the second detector and coincidence events were not registered during tests with alpha sources.

Further developments will include definition of the particles that satisfy the basic coincidence $D_1D_2D_3$, i.e. the coincidence of the signals corresponding to particle flux of all three detectors. Thus the physical and equivalent dose depth distribution inside the phantom, derived by a single particle will be measured.

The flight unit will be tested for charge and energy response at particle accelerators.

The MATROSHKA - R project, including experiments with Liulin-5 will be carried out on the ISS in 2002.

ACKNOWLEDGEMENTS

This work was partly supported by grants (No 5022/1998 and No. TH-1003/2000) from the Bulgarian Ministry of Education and Science.

REFERENCES

[1] G. D. Badhwar, *et al.*, "In -Flight Radiation Measurements On STS-60", *Rad. Meas*. Vol. 26 (1), 1996, pp. 17-34.

[2] G. Horneck, Radiobiological experiments in space: a review, *"Nucl. Tracks Radiat. Meas"*. Vol. 20, 1992, pp. 185-205.

[3] Task Group on the Biological Effects of Space Radiation, "Radiation Hazards to Crews of Interplanetary Missions: Biological Issues and Research Strategies", *National Research Council,* National Academy Press, Washington, DC, 1996.

[4] V.M. Petrov, A.V. Shafirkin, V. A. Shurshakov, "Radfiation Risk for Long-term Space Flights: a Conceptual Approach and Practical Usage", in *Proc. of the International Workshop on Responses to Heavy Particle Radiation 1998,* Chiba, Japan, 9-10 July, 1999, pp.33-428.

[5] V. M. Petrov, "Investigation of radiation environment dynamics in Russian segment of ISS and on its trajectory and dose accumulation inside and outside station (Project MATROSHKA-R*)", Proc. of 1st International Workshop on Space Radiation Research and 11st Annual NASA Radiation Health Investigators Meeting*, Arona, Italy, 28-31 May, 2000, in press.

[6] Ts. Dachev, *et al*, "Analysis of The Pre-Flight and Post-Flight Calibration Procedures Performed on the Liulin Space Radiation Dosimeter", *Acta Astronautica*, vol. 42, Nos. 1-8, 1998, pp. 375-387.

[7] J. Semkova, et al, "Proposal For A New Radiation Dose Control System For Future Manned Space Flights", *Acta Astronautica*, vol. 36, Nos 8-12, 1995, pp 629-638.

[8] J Semkova, P. Baynov, R. Koleva, J. Miller, "Solid State Dosimetric Telescope for Space Radiation Measurements. Description and Parameters", in *Proc. of the Fifth National Conference with International Participation on Main Problems of Solar-Terrestrial Influences*, Sofia, Bulgaria, 1998, pp. 83-84.